ECASIA special issue paper

SURFACE and INTERFACE ANALYSIS

Received: 24 September 2015 Revised: 4 January 2016 Accepted: 8 January 2016 Published online in Wiley Online Library: 11 February 2016

(wileyonlinelibrary.com) DOI 10.1002/sia.5948

A comparison of ERBS spectra of compounds with Monte Carlo simulations

M. Vos,[a]* G. G Marmitt[b] and P. L. Grande[b]

Electron Rutherford backscattering measures the near-surface composition of samples quantitatively. For interpretation, one usually relies on the single-scattering approximation. Here, we present results for four compounds, containing oxygen and other species, varying from very light to very heavy. Two Monte Carlo codes are described that model these measurements. From these simulations, it is clear that for all samples, multiple scattering occurs frequently, but also that the single scattering interpretation deduces the right composition, except for O atoms in a very heavy matrix, where interpretation is more difficult. The intrinsic width of the peaks, a consequence of Doppler broadening due to the velocity of the (vibrating) atoms, turns out to be more sensitive to multiple scattering effects.

Keywords: electron Rutherford backscattering; Monte Carlo simulations; elastic scattering

Introduction

The analysis of the elemental composition of the near-surface area is routinely required in surface science and nanotechnology. The two techniques that are most frequently used for this are X-ray photo electron spectroscopy (XPS) and (ion) Rutherford backscattering spectrometry (RBS). Each of these techniques has its own merits. XPS is extremely surface-sensitive and often requires surface preparation in order to acquire meaningful information. RBS measures a thicker layer and relies on well-established cross sections, which makes it ideal for fully-quantitative measurements.

In recent years, another technique has been suggested: electron Rutherford backscattering (ERBS).[1] It relies just as RBS on elastic collisions with well-established cross sections, but in ERBS, an electron scatters from a target atom. Because of the large mass mismatch of the electron and an atom, the fraction of the energy transferred in such a collision is much smaller than in ion scattering. However, electron spectroscopy can be carried out with sub-eV resolution; and hence, it is still possible to resolve many elements. Some authors refer to this technique as elastic peak electron spectroscopy,[2] an acronym that is also used for experiments that compare the elastic peak intensity of different materials with the extract inelastic mean free path (IMFP).[3]

Just as in XPS, the inelastic mean free path of electrons determines in ERBS the depth of the sample probed. As it uses usually higher kinetic energy electrons (40 keV vs $\approx$ 1 keV for XPS) it is less surface sensitive. In this paper, the potential of this technique is demonstrated by comparing the spectra of four very different O-containing samples: one sample consisting solely of light atoms, and others contain medium and high-Z elements. Their ERBS spectra differ greatly, as can be seen in Fig. 1. How precise can one determine the composition? The answer to this question will vary from sample to sample, and the main factors that determine the outcome are:

- how well are the peaks of different elements separated,
- is there any background under the peaks that is poorly understood,
- is the single scattering approximation fully justified.

The last point deserves some explanation, as it is the main topic of this paper. In the experiments, one measures electrons backscattered from the sample into the analyser. In the single scattering case, where the projectile interacts with only one target atom, one can calculate the transferred energy to the atom easily: if the change of momentum of the projectile is q then the transferred (recoil) energy to the (stationary) scattering atom E_{rec} is simply $E_{rec} = q^2/2M$ with M the mass of the scattering atom. If the electron is scattered more than once, possibly from different elements, then the total energy transferred from the projectile to the target is much harder to predict. Here, we use Monte Carlo techniques to investigate the contribution of multiple collisions to the spectrum and determine when their presence affects the outcome of the experiment. Monte Carlo methods have been used in the past to simulate an ERBS experiment from carbon films.[4] There, a small influence of multiple scattering on the observed width of the carbon peak was found. Alvarez and Yubero simulated the ERBS results for polyethylene using Monte Carlo methods and concluded some influence of multiple scattering on the peak width and deduced sample composition.[5] Li *et al.* simulated an earlier version of the experiment, employing

* *Correspondence to: M. Vos, Atomic and Molecular Physics Laboratory, Australian national university. E-mail: maarten.vos@anu.edu.au*

a *Atomic Molecular Physics Laboratories, Research School of Physics Engineering, Australian National University, Canberra ACT Australia*

b *Instituto de Fisica da Universidade Federal do Rio Grande do Sul, Avenida Bento Goncalves 9500, 91501-970 Porto Alegre, RS, Brazil*

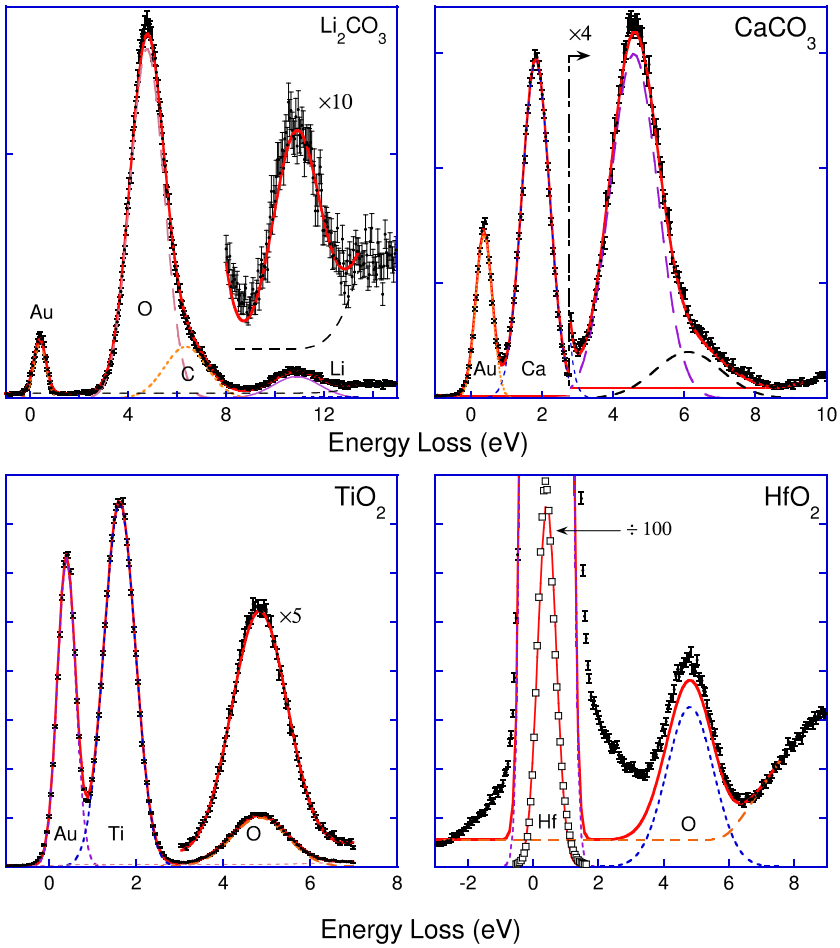

Figure 1. The electron Rutherford backscattering spectra taken of Li_2CO_3, $CaCO_3$, TiO_2 and HfO_2. On the first three samples, a small amount of Au was evaporated, to establish the energy resolution and the zero of the energy scale.

smaller scattering angles using Monte Carlo methods.[6] Here, we study compounds consisting of heavier atoms.

Experimental results

The experiments have been described extensively elsewhere.[7] In brief, electrons with a kinetic energy of 40 keV impinge on a material and electrons scattered over $\theta = 135°$ are detected by an electrostatic analyser. The energy resolution of the system is $\approx$ 0.35 eV. A two-dimensional detector is used to improve the count rate. Good quality spectra are obtained in 1–2 h, using a beam current of 5–10 nA. The beam spot is 0.2 mm diameter.

The resulting spectra are shown in Fig. 1. The carbonate samples consisted of a powder pressed in a pill. The TiO_2 sample was obtained by thermal oxidation of Ti foil. The HfO_2 sample was a 60 nm thick HfO_2 layer grown by atomic layer deposition on a silicon wafer. Results of these films were published elsewhere;[8–10] here, the focus is on the investigation of the influence of multiple scattering on the experiment, as well as an illustration of how ERBS can be used to determine the sample composition for a wide range of samples.

Often, it is helpful to evaporate a thin layer of Au on the sample. This was performed for Li_2CO_3 ($<$ 1Å), $CaCO_3$ and TiO_2 (both $\approx$ 2 Å). The Au peak is narrow and serves as a check of the spectrometer performance and helps determining the exact zero point of the energy scale. It is clear from the figure that the contribution of other elements is broader. This is due to lattice vibrations: the energy transferred by the projectile electron to the atom depends on the velocity of the atom just before the collision. This is a case of Doppler broadening. The Doppler width σ_D^i of the element i can be related to the mean kinetic energy E_{kin}^i of the scattering atom [4]:

$$\sigma_D^i = \sqrt{\frac{4}{3} E_{\text{kin}}^i E_{\text{rec}}^i} \qquad (1)$$

The four spectra shown in Fig. 1 are very different. For Li_2CO_3, the main peak is due to oxygen. This peak is asymmetric because of the contribution of electrons scattered from C atoms, which is not fully resolved. Li is seen as a small peak near 11 eV. The Li peak is not completely free from a background, which rises sharply near 12 eV. This is due to electrons scattered elastically from O atoms who also created an electron-hole pair. Details about the fitting procedure and the determination of the band gap and mean kinetic energy of the atoms can be found elsewhere.[10,11] For $CaCO_3$, the carbonate part of the elastic peak is very similar to that in Li_2CO_3, but now most intensity is due to Ca near 2 eV energy loss.

The other two samples are oxides: TiO_2 and HfO_2. The fitting of the TiO_2 spectrum is straightforward. The HfO_2 case is much more complicated. The Hf peak is huge, and electrons scattered elastically from Hf but also created an electron-hole pair cause a rise

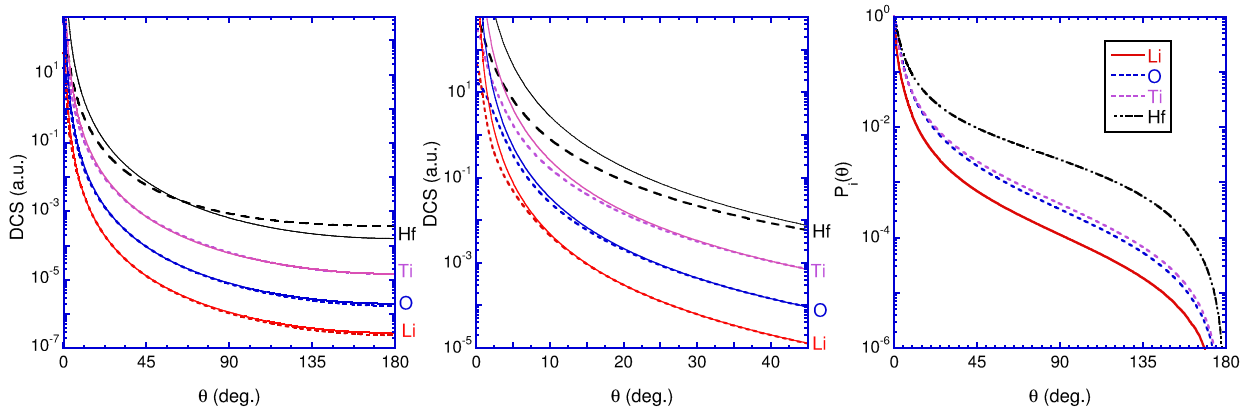

Figure 2. Differential elastic cross section at 40 keV for several elements relevant for this paper (dashed line: partial wave results, full line: Rutherford cross section). The central panel is for forward angles only. The right panel shows the fraction of collisions *exceeding* a certain angle for the partial wave calculation.

in the background from 6 eV onwards. In addition, the Hf peak is not 100% Gaussian and additional tails, extending both at the low and high energy loss side of the peak, complicate the fitting. Here, we just show the expected shape of the Hf and O elastic peak plus background because of inelastic losses.

Monte Carlo simulations

The spectra obtained in these experiments are a result of two interplaying processes. One is deflection from the incoming electron from the nuclei (referred to as elastic scattering as the sum of the kinetic energy of the electron and scattering atom is conserved). The other is the loss of energy because of electronic excitations (or inelastic scattering). At these high energies, the inelastic excitations do not significantly affect the direction of propagation of the fast electron. As a consequence, one can separate the problem in two parts: calculation of trajectories of elastically scattered electrons for which the electron emerges from the target propagating towards the detector. If such a trajectory is found, than we need to consider the probability that it contributed to the elastic peak, i.e. that there were no inelastic excitations created for this trajectory (with length L). This probability is given by $e^{-L/\lambda_{in}}$ with λ_{in} the IMFP.

Elastic cross sections are usually assumed to be very similar for a free atom and an atom in the condensed phase. In this approximation, differential elastic cross sections (DCS) and the elastic mean free path can be calculated using partial-wave expansion theory, as implemented, e.g. in ELSEPA, [12] which is used here. Examples of elastic cross sections at 40 keV are shown in Fig. 2. For the lighter elements, the partial-wave calculation results are very similar to the Rutherford cross section at larger angles. At forward angles, the partial-wave cross section is smaller, because of screening of the nuclear charge by the bound electrons. For Hf, the partial-wave cross section is substantially larger at backward angles than the Rutherford one. The cause of this is discussed elsewhere, [8] and for Hf, the term 'electron Rutherford backscattering' is not strictly appropriate.

Integrating the elastic DCS over 4π, one obtains the total elastic cross section, σ^i_{el} of atom i. It is instructive to calculate for element i, the fraction of elastic collisions $P_i(\theta)$ for which the scattering angle is *larger* than θ. This is carried out in the right panel of Fig. 2. Only a minute fraction of the scattering events results in deflections larger than 90° ($\approx 10^{-4}$ for Li, but $\approx 5\,10^{-3}$ for Hf). Most deflections have only a very minor effect on the direction of propagation. A quantity that reflects the influence of the scattering event on the propagation direction is the differential transport cross section σ^i_{tr}, the elastic DCS weighted by $(1-\cos\theta)$.

From σ^i_{el}, one can calculate the elastic mean free path λ_{el} in a compound:

$$\frac{1}{\lambda_{el}} = \sum_i n_i \sigma^i_{el} \tag{2}$$

with n_i the concentration of element i. An equivalent expression gives the transport mean free path λ_{tr}, a quantity that can be loosely interpreted as the distance an electron travels after which the final propagation direction is not correlated any more with the initial one. These quantities are given in Table 1 for the compounds studied here, together with λ_{in} as calculated in the Tanuma–Powell–Penn approach. [13] Note the sharp decrease of λ_{el} and in particular λ_{tr} for compounds with heavier atoms. The single scattering approximation should thus be much better for compounds of light elements compared with heavy elements.

The Monte Carlo procedure used here is rather standard. [14,15] It considers only elastic scattering events. Unless otherwise stated the random numbers R_i are homogeneously distributed between 0 and 1. The distance S to the next scattering event is determined by:

$$S = -\lambda_{el} \ln R_1 \tag{3}$$

The next random number R_2 decides from which atom one scatters. For a ternary sample, one scatters from element 1 if $R_2 < n_1\sigma^1_{el}/\left(n_1\sigma^1_{el} + n_2\sigma^2_{el} + n_3\sigma^3_{el}\right)$, from element 3 if $R_2 > 1 - n_3\sigma^3_{el}/\left(n_1\sigma^1_{el} + n_2\sigma^2_{el} + n_3\sigma^3_{el}\right)$ and otherwise from element 2.

Table 1. The IMFP, EMFP and transport mean free path for the compounds investigated. All quantities are in nm. The IMFP was obtained from the TPP-2 formula, the EMFP and transport mean free path are based on ELSEPA calculations of the elastic scattering cross section for (neutral) atoms and nominal density of the atoms.

Sample	λ_{in}	λ_{el}	λ_{tr}
Li_2CO_3	58	63	16300
$CaCO_3$	51	30.3	7230
TiO_2	45	18.4	3870
HfO_2	35	8.8	690

IMFP, inelastic mean free path; EMFP, elastic mean free path; TPP, Tanuma–Powell–Penn.

To determine the scattering angle of the next collision, one considers the curve $P_i(\theta)$ as given in the right panel of Fig. 2. The scattering angle is then the θ value for which $R_3 = P_i(\theta)$. The ϕ value for the collision is taken to be $2\pi R_4$.

For each elastic deflection, the recoil loss was calculated in two different ways, assuming that the atom was stationary before the collision:

$$E_{\text{recoil}} = \frac{q^2}{2M_i} = \frac{(2k_0 \sin(\theta_{\text{scat}}/2))^2}{M_i} \quad (4)$$

with k_0, the magnitude of momentum of the impinging electron, and assuming that the atom was moving:

$$E_{\text{recoil}} = \frac{q^2}{2M_i} + \Delta_{Doppler} \quad (5)$$

with $\Delta_{Doppler}$ (positive or negative) determined using a random number taken from a Gaussian distribution with width σ_D^i (Eqn 1, the mean kinetic energy of the atoms, used here in the Monte Carlo (MC) calculation were close to the value extracted from the experiment using the single scattering interpretation or a theoretical estimate). After each deflection, the new direction of propagation is determined, and the procedure is repeated for the next elastic deflection

Two simulation techniques were used. The 'direct' method is described first. In this method, the simulation of a trajectory is stopped when either the trajectory length exceeds $10\lambda_{\text{in}}$ or the electron emerges from the surface (next deflection at a depth < 0). If the emerging electron travels within the acceptance range of the analyser, it is used to calculate the loss spectrum. The simulated spectrum, at the element corresponding to the total energy loss value due to all deflections of that trajectory, is increased by an amount proportional to the probability that this trajectory was not affected by inelastic scattering, i.e. $e^{-L/\lambda_{\text{in}}}$ with L the total trajectory length.

The measurement were performed for the incoming beam along the surface normal. The detector measures electrons traveling along the surface of a cone with half-angle 45° (i.e. scattered over 135°), but the detector covers only a fraction of the cone ($\approx$ 10° out of 360°). The angular acceptance in θ_{scat} is very small (0.2°). Simulating the actual experiment is exceedingly slow. The efficiency in the simulation was increased by assuming that the detector accepts all directions along the cone. As the measurement geometry is cylindrical symmetric, this does not introduce errors. Moreover, it was found that the range of θ values could be increased as well without affecting the outcome noticeable, and all electrons appearing between 42.5° and 47.5° were considered to be detected rather than the actual 0.2° range. A total of 4×10^{10}

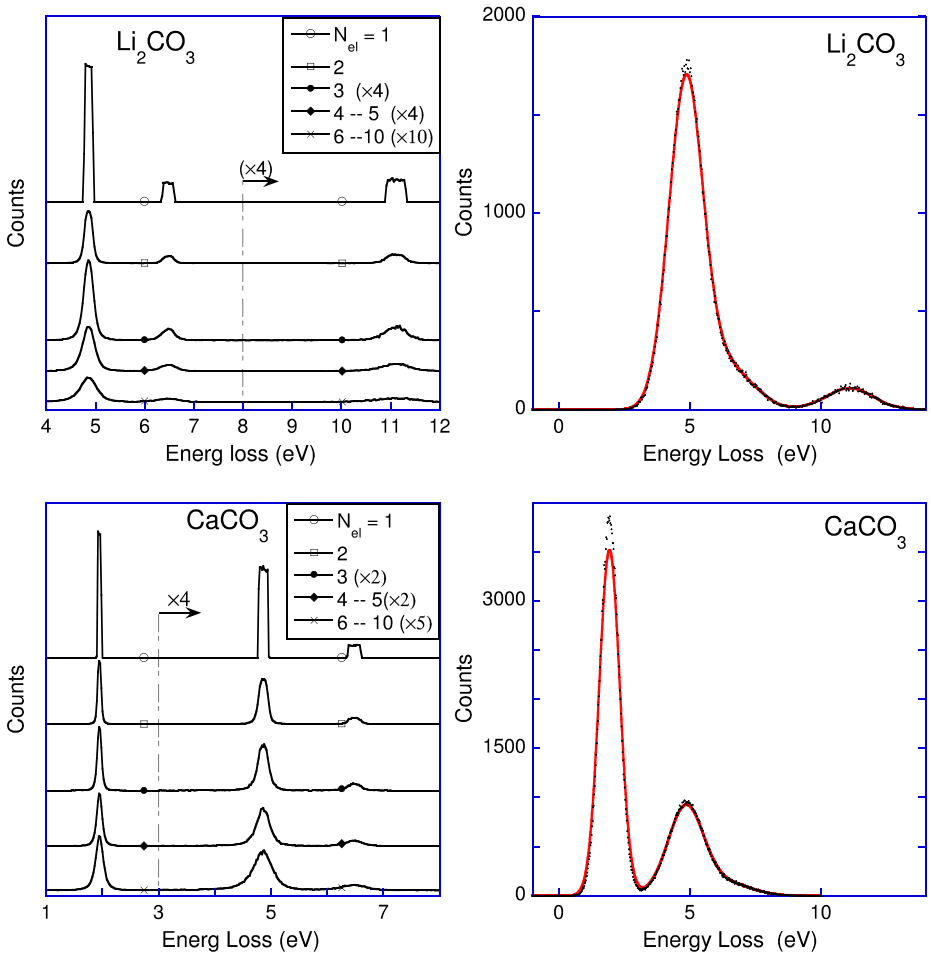

Figure 3. The left panel shows for Li_2CO_3 and $CaCO_3$ the spectra obtained for scattering from stationary atoms, split up for the number of elastic collisions for a detected trajectory. The right panel shows the total spectrum as simulated with Doppler broadening (dots) and after subsequent convolution with the energy resolution of the experiment (line).

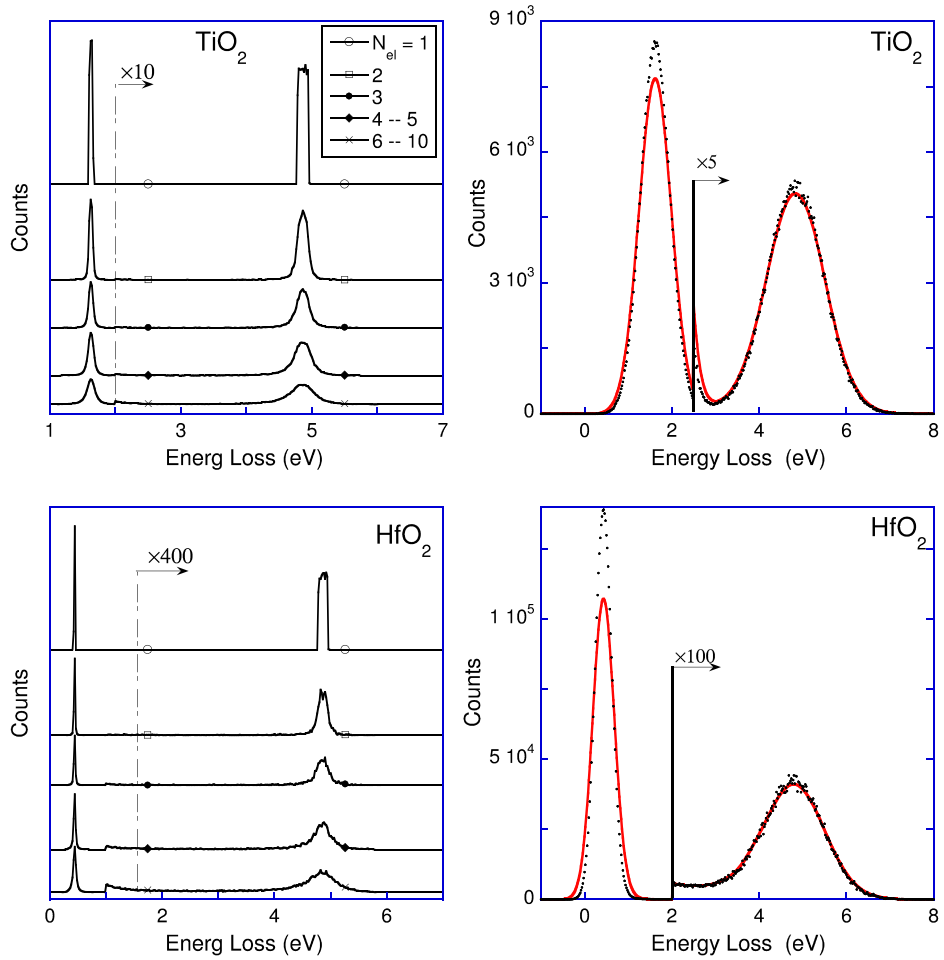

Figure 4. Same as Fig. 3 but now for TiO_2 and HfO_2.

trajectories were simulated, which takes 4 days on a single core of a modern PC for Li_2CO_3 but four times longer for HfO_2 (scales as $\lambda_{in}/\lambda_{el}$).

In order to improve the simulation speed, a second method, the 'connected trajectory' approach, was used as well. Instead of constructing the whole trajectory, incoming and outgoing segments were simulated separately and then connected in a spatial grid. The incoming segment is straightforward; the particles hit the sample along the specified direction. For the outgoing segment, a time reversal technique is used, namely, the particles approaching the sample from the direction of the detector. Electron energy, direction and trajectory path length are stored for each point of the grid. Events without elastic collisions are also stored on the grid. At the connection, the corresponding elastic cross section at a given angle determined from both directions is used to weight the contribution of this trajectory. In addition, the contribution is again weighted by $e^{-L/\lambda_{in}}$.

About 10^7 segments were simulated independently, and they are connected by sampling one incoming and outgoing segments, which correspond to a total of 5×10^8 connections at each grid point. For each sample, a total of 5×10^{10} trajectories were simulated, which takes about 1 hr on an 8 core modern PC.

For both approaches, the result of the simulation was stored in the form of two spectra: one with and one without Doppler broadening. The first can be compared with the experiment, but the second gives insight in how multiple scattering affects the spectrum, as in this case, the results are not 'washed out' by Doppler broadening. The spectra without Doppler broadening are sorted by the number of elastic deflections (N_{el}) of the trajectory. Results are shown in Figs 3 and 4.

For the trajectories with only one elastic deflection, the single scattering interpretation is correct. For this group, the spectra without Doppler broadening have a very sharp onset and drop off, this shape is due to the variation in the recoil energy within the range of θ values covered by the detector.

For trajectories with two deflections, the contribution to the spectrum broadens somewhat. The slow broadening can be understood if one realises that almost always one of the deflections will be very small, and thus, the total recoil energy is very close to the recoil of the one large-angle deflection. The broadening increases with the number of deflections. The intensity of higher-order contributions decreases slowly with the number of deflections, especially when heavy elements are present, Fig. 5. The single scattering contribution was 50% of the total for Li_2CO_3, 36% for $CaCO_3$, 28% for TiO_2 and 19% for HfO_2.

The spectra obtained with Doppler broadening are much wider but are still somewhat 'noisy'. For the simulated spectra, the experimental resolution has not been taken into account. Convoluting the simulated spectra with the experimental energy resolution (taken to be 0.37 eV full-width, half maximum here) broadens the elastic peak of the heavier elements somewhat and averages out the noise that was still visible in the simulation everywhere.

It is immediately clear that the effect of multiple scattering will be small, and the simulated spectra resemble superficially the measured ones with the exception of the contributions affected by inelastic excitations, which were not considered in the simulations.

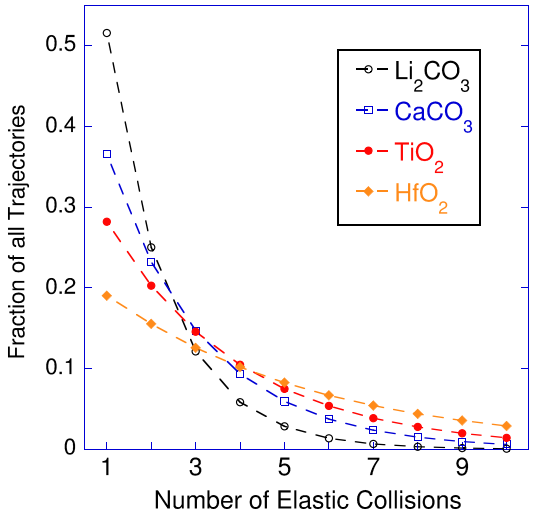

Figure 5. The likelihood of trajectories with a given number of deflections contributing to the elastic peak as determined by the Monte Carlo simulations.

Now, we treat the result of the Monte Carlo simulations (including Doppler broadening and after convolution with the spectrometer resolution) as we normally analyse the experimental data (i.e. assuming single scattering), and fit the results with Gaussians of unknown area and width. From the obtained areas, we infer the stoichiometry. In this way, it becomes evident if multiple scattering changes the apparent stoichiometry. As is seen in Table 2, the obtained stoichiometry is (with a caveat for HfO_2, discussed later) within 1–2.5% the same as the actual stoichiometry, and the quality of the fit was good. From the width of the Gaussians (treating the spectrometer resolution as a known quantity), we can infer the mean kinetic energy of the atoms. Here, there are significant

Table 2. The stoichiometry obtained for the compounds as indicated by fitting the output of the MC calculation and by fitting the actual experiment (exp.). The last column shows the incoming energy E_0 (in eV) as inferred from the MC results. The results were obtained using the 'direct' method and are very similar to those from the connected trajectory method.

Sample	Composition from MC	Composition from exp.	E_0 retr.
Li_2CO_3	2:1.01:3.00	2:0.90:2.86	39875
$CaCO_3$	1:1.01:3.01	1:1.2:3.0	39740
TiO_2	1:2.00	1:1.96	39723
HfO_2	1:2.05*	1:2.0±0.2*	39660

MC, Monte Carlo.

Table 3. The kinetic energy (in meV) used as input for the MC simulations compared with those obtained from fitting of the MC simulated spectra, as obtained for both the 'direct' and 'connected trajectory' method.

Sample	Cation			O			C		
	Input	Direct	Connect	Input	Direct	Connect	Input	Direct	Connect
Li_2CO_3	51.0	55.5	53.9	60.5	62.2	61.4	99.0	101.1	101.1
$CaCO_3$	48.0	49.6	49.2	63.4	68.1	66.3	91.4	98.0	99.1
TiO_2	50.0	52.2	51.5	60.0	66.7	65.2	—	—	—
HfO_2	60.0	61.1	61.5	60.0	83.8	81.6	—	—	—

MC, Monte Carlo.

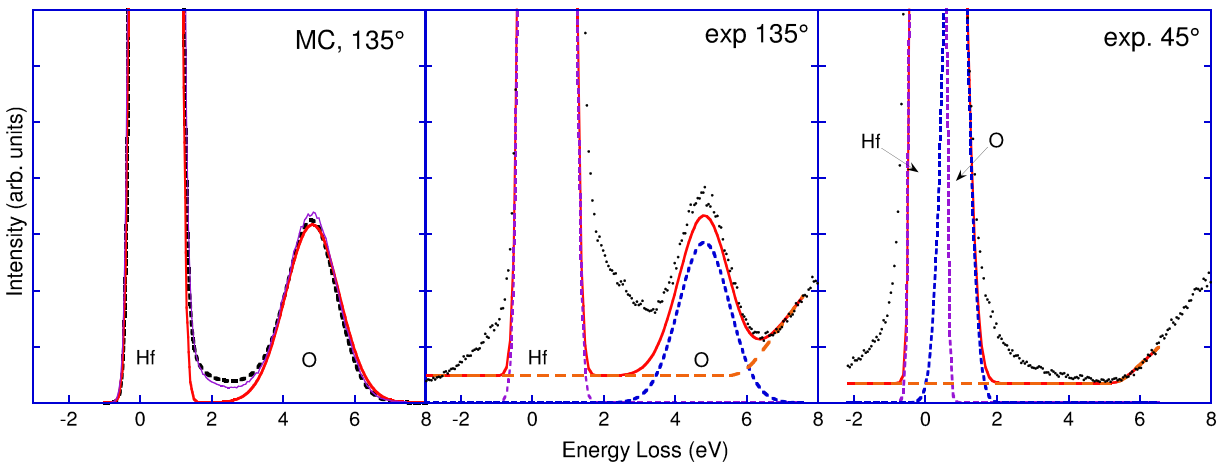

Figure 6. The left panel shows output of the MC calculation (direct method dashed line, connected trajectory method thin line) of HfO_2 and a fit based on two Gaussians (thick line). The centre panel shows experimental and calculated electron Rutherford backscattering spectrum based on the single scattering approximation. The right panel shows the same, but now with a scattering angle of 45° rather than 135°.

differences. The kinetic energy as obtained from the simulation is always larger than the value used as input for the simulation (see table 3). It varies from 4% for the cations to 10% for O in TiO_2 to 40% for O in HfO_2. The extraction of the width of the C component is more difficult, as its peak is the smaller of two partly overlapping peaks. Note that due to the square root dependence of the width on the mean kinetic energy (Eqn 1), a 10% increase in width causes a 20% increase in kinetic energy.

The actual mean kinetic energies obtained from the experiment for the carbonates (including corrections for multiple scattering based on MC simulations and compared with theory) are given in Vos et al. (2015b)[10] for the carbonates. For TiO_2, we found, neglecting multiple scattering, a mean kinetic energy of 50 meV for Ti and 60 meV for O [9]. Based on these MC simulations, we conclude that a better estimate of the mean kinetic energy is 48 meV for Ti and 53 meV for O.

For TiO_2 and the carbonates, the fit of the MC results with Gaussians was very good, but for HfO_2 this is not the case, as is seen in Fig. 6. There is a significant amount of intensity in between the Hf and O peak, which is not reproduced by the fit. As the cross section of Hf is so huge, the probability of a large-angle deflection from Hf in combination with one from O is not small any more compared with the probability of single-scattering from O, causing extra intensity at intermediate losses. Is this observation supported by the experiment? To answer this, we show the experimental result for scattering over 135° (central panel) as well as for scattering over 45° (right panel). The comparison is complicated by the presence of intensity because of electron-hole creation *and* the fact that the response of the analyser is not purely Gaussian: it has some 'Lorentzian' type wings. In the experimental spectra, we also show the expected intensity for HfO_2 assuming Gaussian detector response and a band gap of HfO_2 of 5.4 eV. For the 45° measurement, the recoil is much smaller, and the contribution of the electrons scattered from O is seen as a shoulder. The relative intensity of O is now larger, as at 45° the DCS of Hf is less than Rutherford, whereas at 135° it is larger. In the 45° case, the wings of the Hf peak are quite symmetrical, but for the 135° case, there is more intensity 2 eV below the Hf peak compared with 2 eV below. Thus there is support in the experiment for extra intensity in between the Hf and O peak.

During the fitting of the MC results, the kinetic energy of the incoming beam is a free parameter. The retrieved value is shown in the last column of Table 2. It is always less than the value used in the calculation (40 000 eV), and the differences increases for the heavier targets. Thus there is a very small tendency (reaching 1% for HfO_2) for the separation of the elastic peak to decrease because of multiple scattering. In the experiment, larger effects are seen, but these are attributed to electron beam-induced charging of the targets (here, insulators) up to a few keV.

Conclusion

It was demonstrated that ERBS can obtain the composition of compounds with high accuracy, from 1–2% error for favourable cases (TiO_2 or Ca : O ratio in $CaCO_3$) to 5–20% for more difficult cases where there is a large mismatch in intensity or where there are background issues (Li in Li_2CO_3 or O in HfO_2), or not fully resolved peaks (C in carbonates).

Monte Carlo simulations have shown that multiple scattering hardly affects the obtained stoichiometry for compounds consisting of light and intermediate-*Z* elements, but for compounds containing a large concentration of high-*Z* elements, the effect is somewhat larger. The outcome of the simulation for HfO_2 is in-line with experimental observations of an excess intensity in between the Hf and O peak, but interpretation is complicated by lack of knowledge of the exact shape of the elastic peak of Hf atoms, which exceeds that of O atoms by two orders of magnitude.

The simulations indicate that the peak width (and hence, extracted value of the mean kinetic energy of the atoms) is more sensitive to multiple scattering and the sensitivity increases when higher *Z* elements are part of the compound. For the precise extraction from the mean kinetic energy of atoms, a Monte Carlo simulation is required to correct for multiple scattering effects, but the procedure becomes questionable for cases containing light and very heavy elements, such as HfO_2, where the effect of multiple scattering cannot just be described as a broadening but causes a significant change in the shape of the structure.

Acknowledgements

This work is made possible by a grant of the Australian Research Council. G. G. M acknowledges support from CNPq: Conselho Nacional de Desenvolvimento Científico e Tecnológico - Brazil.

References

[1] M. Went, M. Vos, *Appl. Phys. Lett* **2007**, *90*, 072104.
[2] G. Gergely, M. Menyhard, Z. Benedek, A. Sulyok, L. Köver, J. Toth, D. Varga, Z. Berenyi, and K. Tokesi, *Vacuum* **2001**, *61*, 107.
[3] A. Jablonski, C. Powell, *Surf. Sci* **2004**, *551*, 106.
[4] M. Vos, R. Moreh, K. Tokesi, *J. Chem. Phys* **2011**, *135*, 024504.
[5] R. Alvarez, F. Yubero, *Surface and Interface Analysis* **2014**, *46*, 812.
[6] Y. G. Li, Z. M. Zhang, S. F. Mao, Z. J. Ding, *J. Phys. Condens. Matter* **2008**, *20*, 355005.
[7] M. Went, M. Vos, *Nuclear Instruments and Methods in Physics Research Section B* **2008**, *266*, 998.
[8] P. L. Grande, M. Vos, *Phys. Rev. A* **2013**, *88*, 052901.
[9] M. Vos, P. Grande, *Nuclear Instruments & Methods B* **2015**, *354*, 332.
[10] M. Vos, G. Marmitt, Y. Finkelstein, R. Moreh, *Journal of Chemical Physics* **2015**, *143*, 104203.
[11] G. Marmitt, L. Rosa, S. Nandi, M. Vos, *J. Electron Spectrosc. Relat. Phenom.* **2015**, *202*, 26.
[12] F. Salvat, A. Jablonski, C. J. Powell, *Comput. Phys. Commun* **2005**, *165*, 157.
[13] S. Tanuma, C. J. Powel, D. R. Penn, *Surf. Interface Anal* **1993**, *20*, 77.
[14] R. Shimizu, Z.-J. Ding, *Rep. Prog. Phys* **1992**, *55*, 487.
[15] M. Dapor, *Transport of Energetic Electrons in Solids. Computer Simulation with Applications to Materials Analysis and Characterization*, Springer-Verlag, Berlin, **2014**.